Taylor & Francis
Taylor & Francis Group

Journal of Toxicology and Environmental Health, Part A
Current Issues

ISSN: 1528-7394 (Print) 1087-2620 (Online) Journal homepage: http://www.tandfonline.com/loi/uteh20

Characterization of pulmonary responses in mice to asbestos/asbestiform fibers using gene expression profiles

Naveena Yanamala, Elena R. Kisin, Dmitriy W. Gutkin, Michael R. Shurin, Martin Harper & Anna A. Shvedova

To cite this article: Naveena Yanamala, Elena R. Kisin, Dmitriy W. Gutkin, Michael R. Shurin, Martin Harper & Anna A. Shvedova (2018) Characterization of pulmonary responses in mice to asbestos/asbestiform fibers using gene expression profiles, Journal of Toxicology and Environmental Health, Part A, 81:4, 60-79, DOI: 10.1080/15287394.2017.1408201

To link to this article: https://doi.org/10.1080/15287394.2017.1408201

View supplementary material

Published online: 26 Dec 2017.

Submit your article to this journal

Article views: 79

View related articles

View Crossmark data

Full Terms & Conditions of access and use can be found at
http://www.tandfonline.com/action/journalInformation?journalCode=uteh20

Download by: [Stephen B. Thacker CDC Library] **Date:** 11 January 2018, At: 09:00

JOURNAL OF TOXICOLOGY AND ENVIRONMENTAL HEALTH, PART A
2018, VOL. 81, NO. 4, 60–79
https://doi.org/10.1080/15287394.2017.1408201

Taylor & Francis
Taylor & Francis Group

Check for updates

Characterization of pulmonary responses in mice to asbestos/asbestiform fibers using gene expression profiles

Naveena Yanamala[a], Elena R. Kisin[a], Dmitriy W. Gutkin[b], Michael R. Shurin[b], Martin Harper[a,c], and Anna A. Shvedova[a,d,e]

[a]Exposure Assessment Branch, NIOSH/CDC, Morgantown, WV, USA; [b]Department of Pathology, University of Pittsburgh Medical Center, Pittsburgh, PA, USA; [c]Zefon International, Inc., Ocala, FL, USA; [d]Department Physiology, Pharmacology & Neuroscience, School of Medicine, West Virginia University, Morgantown, WV, USA; [e]Department of Pharmaceutical Sciences, School of Pharmacy, West Virginia University, Morgantown, WV, USA

ABSTRACT

Humans exposed to asbestos and/or asbestiform fibers are at high risk of developing many lung diseases including asbestosis, lung cancer, and malignant mesothelioma. However, the disease-causing potential and specific metabolic mechanisms and pathways associated with various asbestos/asbestiform fiber exposures triggering different carcinogenic and non-carcinogenic outcomes are still largely unknown. The aim of this this study was to investigate gene expression profiles and inflammatory responses to different asbestos/asbestiform fibers at the acute/sub-acute phase that may be related to delayed pathological outcomes observed at later time points. Mice were exposed to asbestos (crocidolite, tremolite asbestos), asbestiform fibers (erionite), and a low pathogenicity mineral fiber (wollastonite) using oropharyngeal aspiration. Similarities in inflammatory and tissue damage responses, albeit with quantitative differences, were observed at day 1 and 7 post treatment. Exposure to different fibers induced significant changes in regulation and release of a number of inflammatory cytokines/chemokines. Comparative analysis of changes in gene regulation in the lung on day 7 post exposure were interpretable in the context of differential biological responses that were consistent with histopathological findings at days 7 and 56 post treatment. Our results noted differences in the magnitudes of pulmonary responses and gene regulation consistent with pathological alterations induced by exposures to four asbestos/asbestiform fibers examined. Further comparative mechanistic studies linking early responses with the long-term endpoints may be instrumental to understanding triggering mechanisms underlying pulmonary carcinogenesis, that is lung cancer versus mesothelioma.

Downloaded by [Stephen B. Thacker CDC Library] at 09:00 11 January 2018

Introduction

Asbestos is a term for a set of commercially important naturally occurring fibrous silicate minerals. Crocidolite (asbestiform riebeckite), amosite (asbestiform cummingtonite-grunerite), actinolite-tremolite asbestos, and anthophyllite asbestos belong to the amphibole minerals, while chrysotile is a serpentine mineral (Wylie and Candela 2015). The term "asbestiform" corresponds to a mineralogical habit or form of a mineral in which single fibers (fibrils) occur in bundles that can be detached into finer fibers and display curvature (Lowers and Meeker 2002). Similar to main asbestos types described above, there are "other regulated asbestiform minerals" fibers such as durable asbestiform zeolite minerals (e.g., erionite). The term asbestos has been used in commerce and regulations, but is not recognized in geology as referring to species separate from non-asbestos analogs of these minerals (Lowers and Meeker 2002). These materials were widely used for textiles and in construction, as well as in industrial application, until the 1970's in the USA (Williams, Phelka, and Paustenbach 2007). Although the use has declined, asbestos continues to be utilized for certain applications in the USA and elsewhere (Dodson 2016; LaDou et al. 2010). Known human diseases associated with exposure to asbestos/asbestiform fibers include asbestosis, bronchial adenocarcinoma, squamous cell carcinoma of the respiratory epithelium and large/small cell lung carcinoma and diffuse malignant mesothelioma (Andujar et al. 2016; Lemen 2016; Ndlovu et al. 2017).

CONTACT Anna A. Shvedova ats1@cdc.gov Exposure Assessment Branch (MS-3030), 1095 Willowdale Road, Morgantown, WV 26505, USA
Color versions of one or more of the figures in the article can be found online at www.tandfonline.com/uteh.
The supplemental data for this article can be accessed here.
This article not subject to U.S. copyright law.

Downloaded by [Stephen B. Thacker CDC Library] at 09:00 11 January 2018

Both carcinogenic and non-carcinogenic health outcomes such as pleural fibrosis and plaques, pulmonary fibrosis, have been observed in asbestos workers. Much of our understanding regarding the mechanisms for induction of carcinogenic and non-carcinogenic outcomes is based upon studies involving the biological effects of asbestos/asbestiform fibers (Kane 1996; Oberdorster 1996; Sanchez et al. 2009; Sayan and Mossman 2016). The disease-causing potential of asbestos related exposures is governed by several factors, including (1) duration and frequency of exposures, (2) individual susceptibility and biopersistence, as well as (3) type, shape and surface characteristics of the fibers (Fubini and Fenoglio 2007; Kane 1996). However, not all fibers with similar characteristics have the potential to trigger similar pathogenic responses. For example, despite exhibiting almost identical size distributions, erionite and crocidolite asbestos fibers lead to differential carcinogenic outcomes (Andujar et al. 2016; Carbone et al. 2011; Carbone and Yang 2012; Wagner et al. 1985). The inhalation of fibrous erionite by rats produced mesothelioma in 96.6% of animals but no apparent lung cancers (Wagner et al. 1985). Crocidolite (in the same experiment at 10-fold higher dose than erionite) produced lung cancer in 3.6% of rats with no appearance of mesotheliomas. However prolonged exposures to high levels of crocidolite asbestos fibers was reported to induce mesothelioma in approximately 5% of humans, albeit requiring additional factors such as genetic predisposition and/or SV40 infection (Carbone, Kratzke, and Testa 2002; Carbone et al. 1994; Comar et al. 2012; Dogan et al. 2006). Additional individual risk factors, such as smoking and other pre-existing lung diseases, further complicate disease paradigms seen after asbestos exposures. While smoking combined with asbestos exposure did not appear to increase the risk of mesothelioma occurrence (Frost, Darnton, and Harding 2011; O'Reilly et al. 2007), it is known to enhance the risk of developing lung cancer that is greater than the individual risks from asbestos and smoking added together (Moller et al. 2014; NTP 2016). Moreover, both erionite and fibrous talc (asbestiform mineral fibers) are thought to be biopersistent. Yet erionite is a potent animal and human carcinogen while fibrous talc is not (Wild 2006). These studies indicate that morphology, fiber type/size/number and biopersistence are not the only critical factors/indicators that determine fiber-induced carcinogenesis (Boulanger et al. 2014).

Animal models and cellular mechanistic studies have greatly assisted in understanding the basis of various pathologic changes observed during asbestos/asbestiform fiber exposures (Albrecht, Borm, and Unfried 2004; Bernstein et al. 2005; Cyphert et al. 2016; Oberdorster 1996; Singh, Pruett, and Hoang 2017). While previous *in vitro* and *in vivo* studies provide details regarding asbestos-induced toxicity and changes in gene expression, mechanistic investigations comparing different asbestos/asbestiform fibers to define relative risk (RR) of initiating non-carcinogenic and carcinogenic outcomes and developing mesothelioma versus lung cancer remain to be determined. The aim of this study was to assess the ability of a known low-pathogenicity fiber—wollastonite (Maxim and McConnell 2005; McConnell, Hall, and Adkins 1991); high-pathogenicity fibrous erionite (Rome, OR); and two amphibole asbestos fibers—crocidolite (asbestiform riebeckite) and tremolite asbestos to induce inflammation, tissue damage, and histopathological alterations in mouse lung. In order to facilitate early detection of alterations in genes relevant to each exposure as well as to relate such changes to a particular outcome in lungs (before a large number of genes are dysregulated), alterations in gene expression profiles at day 7 post exposure were determined and compared to histopathological outcomes at a later time point (i.e., 56 days). Such approaches are crucial for facilitating early identification of biological molecules that distinguish between different fiber exposures and those that correlate with initiation and/or progression of asbestos-related diseases.

Methods

Characterization of asbestos particles

The structure and dimensions of a known low-pathogenicity fiber wollastonite (Hubei, China); high-pathogenicity erionite fibers (Rome, OR); and two types of asbestos fibers - crocidolite (l' Union Internationale Centre le Cancer, UICC) and tremolite asbestos (Lone Pine, CA; (Harper et al. 2015)) were characterized by transmission electron microscopy (TEM). Asbestos/asbestiform fibers at 1 mg/ml concentration were vortexed to disperse the particles

Downloaded by [Stephen B. Thacker CDC Library] at 09:00 11 January 2018

in solution. A tuberculin syringe was used to withdraw a small amount of the solution, and a drop was casted on a formvar-coated 200 mesh copper grid. The grid was left to dry overnight. Asbestos fibers were imaged using a JEOL 1400 transmission electron microscope (JEOL, Tokyo, Japan) at 80 kV, and an XR81-MB Advanced Microscopy Techniques (AMT) digital camera (Woburn, MA, USA) was utilized to capture the images. Depending upon the length of the fibers in each asbestos/asbestiform samples, varying magnifications were employed to ensure that full lengths of the fibers could be visualized in the imaging field. Higher magnification images of thinner fibers were captured in order to more accurately visualize and measure the width of the fiber. A minimum of 300 fibers per sample ($n = 3$) were counted for accurate characterization of fibers such as length, width and aspect ratio. "Fiber" definition for counting included the criteria of being more than ≥5 μm in length or having ≥ 3:1 aspect ratio.

Animals

C57BL/6J female mice (8–9 weeks) used in these studies were purchased from Jackson Laboratories (Bar Harbor, ME). Specific pathogen-free mice weighing 22 ± 1.9 g were housed individually in cages receiving HEPA-filtered air, and supplied with irradiated NIH-31 modified 6% mouse food (Envigo RMS, Inc.) and water *ad libitum*. Beta Chips (Northeastern Products Corp., Warrensburg, NY) were used for bedding and changed weekly. Animals were acclimated in the animal facility under controlled temperature and humidity for at least one week before exposure. Mice were monitored weekly and weights recorded for each group before treatment and post-treatment periods until the time of euthanasia. All experimental procedures were conducted in accordance with the Guide for the Care and Use of Laboratory Animals, 8th ed. and approved by the National Institute for Occupational Safety and Health (NIOSH) Institutional Animal Care and Use Committee.

Experimental design

Mice were exposed to asbestos/asbestiform materials including erionite, tremolite asbestos, crocidolite and wollastonite. Suspensions of particles (80 μg/mouse, 50 μl) were administered by pharyngeal aspiration to experimental mice while, corresponding control group received sterile USP grade Ca^{2+} and Mg^{2+} free phosphate buffered saline (PBS). The selected dose was based upon our estimated calculations of approximately 8.8×10^7 fibers/mouse (Murray et al. 2012) with >5 μM size comparable to human occupational exposures estimated at 10^{10} – 10^{11} fibers during a lifetime (National Research Council (U.S.). Committee on Nonoccupational Health Risks of Asbestiform Fibers 1984). Briefly, after anesthetization with a mixture of ketamine and xylazine (62.5 and 2.5 mg/kg subcutaneous in the abdominal area), the mouse was placed on a board in a near vertical position and the animal's tongue extended with lined forceps. A suspension of studied materials prepared in USP grade PBS was placed at the base of the tongue, which was held until the suspension was aspirated into the lungs. The mice revived unassisted after approximately 30–40 min. All mice in erionite, tremolite asbestos, crocidolite, and wollastonite-treated experimental and control groups survived this treatment procedure. This technique provided reliable distribution of particles widely disseminated in a peri-bronchiolar pattern within the alveolar region as was reported previously using histopathology (Rao et al. 2003). Animals treated with the particulates or PBS recovered rapidly after anesthesia with no behavioral or negative health outcomes. Mice were sacrificed 1 and 7 days following exposure to assess the inflammatory responses as evidenced by total cell counts and cell differentials, cytokine/chemokine responses, tissue damage assessed by LDH activity test and/or changes in pulmonary gene expression profiles. To further assess how alterations in gene expression profiles at acute/sub-acute phase (e.g., at 7 days) relate to pulmonary outcomes at extended time points of post exposure, additional groups of animals were sacrificed at 7 and 56 days to evaluate histopathological alterations in the lungs. The 7 days post exposure time point, for evaluating gene expression changes, was specifically selected as it is not overwhelmed by initial acute phase responses and fibrosis is not seen yet upon asbestos exposure (Table 3, 7 days).

Downloaded by [Stephen B. Thacker CDC Library] at 09:00 11 January 2018

Bronchoalveolar lavage fluid collection

Mice were weighed and sacrificed with intraperitoneal injection of sodium pentobarbital (>100 mg/kg) and exsanguinated. The trachea was cannulated with a blunted 22 gauge needle, and bronchoalveolar lavage (BAL) was performed using cold sterile PBS at a volume of 0.9 ml for first lavage (kept separate) and 1 ml for subsequent lavages. Approximately 5 ml of BAL fluid per mouse was collected in sterile centrifuge tubes. Pooled BAL cells for each individual mouse were washed in PBS by alternate centrifugation (300 × g, 10 min, 4°C) and resuspension. Cell-free first fraction BAL aliquots were frozen at −80°C until processed.

Cell differentials

The degree of inflammatory response induced by the pharyngeal aspiration exposure to erionite, tremolite asbestos, crocidolite, or wollastonite was determined by quantitating total cells, macrophages, and polymorphonuclear leukocytes (PMN) recovered from the cell pellet fractions of the BAL. After re-suspending cells in 500 µl PBS, total cells were determined using an electronic cell counter equipped with a cell sizing attachment (Coulter model Multisizer II with a 256C channelizer, Coulter Electronics, Hialeah, FL). After estimating the volume needed to normalize for 1×10^5 cells per slide, the cytospin BAL fluid slides were centrifuged at 800 rpm for 5 min on a cytocentrifuge (Cytospin 4, Thermo Fisher Scientific Inc. Waltham, MA, USA). Following this, cellular components were stained with HEMA 3 fixative, solution I, solution II (Fisher Scientific, Kalamazoo, MI). Cytospin slides were analyzed for cell differentials (alveolar macrophages, PMN leukocytes, including eosinophils and lymphocytes) by light microscopy and evaluated using the Olympus CellSens Dimension software (Tokyo, Japan). At least 350 cells per slide were counted for each sample and then corrected for total cells/µl BAL fluid.

Tissue damage

The activity of lactate dehydrogenase (LDH) in BAL fluid was assayed spectrophotometrically using a Synergy H1 Hybrid Reader (BioTek, Winooski, VT). The reduction of nicotinamide adenine dinucleotide in the presence of lactate to pyruvate using a Lactate Dehydrogenase Reagent Set (Pointe Scientific, Lincoln Park, MI) was monitored at 340 nm.

Preparation of lung tissue homogenates

The whole lung was dissected, weighed and homogenized using a tissue tearor (model 985–370, Biospec Prod. Inc., Racine, WI) in cold PBS (pH 7.4, 4°C). The homogenate suspensions were immediately aliquoted and stored at -80°C until further use. All measurements performed using lung homogenates were further normalized by total protein content in each sample. Quantity of total protein in the tissue homogenates was evaluated a modified Bradford assay according to the manufacturer's instructions (BioRad Laboratories, Hercules, CA). The absorbance (595 nm) was measured using a Synergy H1 hybrid multi-mode microplate reader (BioTek Instruments, Inc., Winooski, VT) and protein amount calculated using bovine serum albumin as a standard.

Inflammatory cytokine/chemokine responses

The levels of cytokines, chemokines and growth factors in lung homogenates were measured in exposed or control groups using the Bio-Plex mouse cytokine assay kits (Bio-Rad, Hercules, CA, USA). The concentrations were calculated using Bio-Plex Manager 6.1 software from standard curves.

Preparation of lungs for histopathological evaluations

Briefly, animals were administered a fatal intraperitoneal injection of sodium pentobarbital, once the animal was unconscious, the trachea was cannulated, and laparotomy was performed. Mice were then euthanized by exsanguination. The pulmonary artery was cannulated via the ventricle and an outflow cannula inserted into the left atrium. In quick succession, the tracheal cannula was connected to a 5 cm H_2O pressure source, and clearing solution (saline with 100 U/ml heparin, 350 mM sucrose) was perfused to clear blood from the lungs. The perfusate was then switched to the fixative. Fixed lung volume was measured by water displacement. Coronal sections were cut

Downloaded by [Stephen B. Thacker CDC Library] at 09:00 11 January 2018

from the lungs. The lungs were embedded in paraffin and sectioned at a thickness of 5 μm with an HM 320 rotary microtome (Carl Zeiss, Thornwood, NY). Lung sections for histopathologic evaluation were stained with hematoxylin and eosin or trichrome blue and examined by a board certified pathologist for morphological alterations.

Cluster analysis of cytokine data

In order to group different asbestos/asbestiform materials based upon their cytokine responses, hierarchical cluster analysis was performed. The measured cytokine concentrations at day 1 and 7 post exposure were first converted to fold change compared to their levels in control samples and then $\log_2$-transformed. Cytokines having measurement values below the limit of detection (LOD) were not used in the analysis. Hierarchical agglomerative (bottom up) clustering analysis using R was applied to group control and samples corresponding to different materials employed. The analysis was performed using "Euclidean" distance (Everitt et al. 2011) similarity between different samples and by employing ward.D2 linkage distance (Murtagh and Legendre 2014; Ward 1963) between the members of the clusters. By combining cytokine and sample clustering, heat maps were created with colors corresponding to the relative levels of the cytokines. The heat map and cluster of similar cytokines profiles and samples corresponding to various asbestos/asbestiform fibers studied were produced with package heat map built for R version 3.1.3 (R Development Core Team 2010).

Microarray sample preparation and analysis

Global gene expression for each treatment was determined using high-throughput mRNA microarray analysis following MIAME guidelines (Brazma et al. 2001). Total RNA was isolated from left lung tissues of control and erionite, tremolite asbestos, crocidolite or wollastonite exposed mice 7 days post treatment (n = 3 for each group). The RNA was isolated using TRIzol reagent (Invitrogen, Carlsbad, CA, USA) and purified using RNeasy MiniKits (Qiagen, Mississauga, ON, Canada) as described by the manufacturer. On-column DNase treatment was applied (Qiagen, Mississauga, ON, Canada). Total RNA from each sample was quantified by the NanoDrop ND-1000 and RNA integrity was assessed by standard denaturing agarose gel electrophoresis. All RNA samples showed an absorbance (A260/280) ratio greater than 2.0. Total RNA of each sample was utilized for labeling and array hybridization as the following steps: 1) Reverse transcription with Invitrogen Superscript ds-cDNA synthesis kit; 2) ds-cDNA labeling with NimbleGen one-color DNA labeling kit; 3) Array hybridization using the NimbleGen 12 × 135 K microarray followed by washing with the NimbleGen wash buffer kit; 4) Array scanning utilizing the Axon GenePix 4000B microarray scanner (Molecular Devices Corporation). Scanned images (TIFF format) were then imported into NimbleScan software (version 2.5) for grid alignment and expression data analysis. Expression data were normalized through quantile normalization and the Robust Multichip Average (RMA) algorithm included in the NimbleScan software. The Gene level (*_RMA.calls) files generated after normalization were imported into Agilent GeneSpring GX software (version 12.1) for further analysis. Differentially expressed genes with statistical significance between two groups were identified through Volcano Plot filtering (Li 2012). Genes showing expression changes of at least 2.5-fold in either direction compared to their controls and having p-values of less than or equal to 0.05 ($p \leq 0.05$) were considered significantly differentially expressed and for further analysis. All gene expression data were uploaded to NCBI's Gene Expression Omnibus and are accessible via accession number (GenBank ID: GSE100900).

Enrichment of KEGG pathways and disease-related responses

The Kyoto Encyclopedia of Genes and Genomes (KEGG) enrichment analysis of differentially expressed genes and those with similar gene expression changes in disease versus normal conditions was made using Enrichr (Kuleshov et al. 2016). The prediction of the disease-related alterations in genes with similar expression

Downloaded by [Stephen B. Thacker CDC Library] at 09:00 11 January 2018

perturbations upon exposure to erionite, tremolite asbestos, crocidolite and wollastonite was performed using Crowd module/tool in Enrichr (Kuleshov et al. 2016). A p-value cutoff of ≤0.05 was considered significant in each case.

Functional analysis using ingenuity pathways analysis tool

To identify pathways and signaling networks that are significantly perturbed upon exposure to different asbestos/asbestiform fibers in mice, Ingenuity Pathway Analysis (IPA, ver. 8.6; Redwood City, CA; www.ingenuity.com) was conducted on differentially expressed genes. Tab delimited text files containing gene IDs, expression data, t-test p-values and false discovery rates (FDRs) were uploaded into IPA for conducting a core analysis. A fold change cutoff of 2.5, and p-value < 0.05 was set to identify genes whose expression was significantly differentially regulated in each case. Score rankings for the top canonical pathways and IPA-identified gene signaling networks (GSN) were calculated using IPA-generated negative logarithm p-values that is, -log10 (p-value) and associated Z- and network scores. The estimated Fisher's exact p-values, pathway- and network-activation scores reflect whether the probability or likelihood of genes occurring in a given pathway/biofunction/disease/network versus others is based on pure chance or not.

Statistics

Statistical analysis was performed using SigmaPlot 11.0 (San Jose, CA). Treatment related differences were evaluated using Student's t-test or one-way ANOVA, as appropriate. A $p \leq 0.05$ was considered to be statistically significant. Data are presented as Mean + SE.

Results

Particle characteristics

The characterization of investigated samples indicates the presence of fibers, as defined by OSHA 1926.1101 Standard (more than 5 μm in length and having an aspect ratio more than 3:1) in comparable quantities. While erionite was composed of bundles of fibers, amphibole asbestos fibers—crocidolite and tremolite asbestos—contained a combination of single fibers as well as bundles (Figure 1). The general morphology of erionite mineral fibers was similar to those reported previously (Lowers et al. 2010). Median length, width, and aspect ratio of the fibers—as estimated by TEM analysis—is presented in Table 1. Overall while tremolite and crocidolite exhibited similar median lengths and widths, the wollastonite followed by erionite exhibited overall lower median lengths, higher median widths and smaller aspect ratio compared to the amphibole asbestos fiber materials investigated in this study (Table 1). Of all the fibers investigated, wollastonite exhibited the lowest median aspect ratio (approximately 3.5).

Pharyngeal aspiration exposure to erionite mineral and other amphibole asbestos fibers

To characterize lung injury and inflammatory responses, cell differentials in BAL fluid of exposed mice were determined 24 hr and 7 days post aspiration exposure to erionite, tremolite asbestos, wollastonite, and crocidolite fibers. While levels of total cells remained at control levels at 24 hr post treatment to different fibers investigated, a significant increase was observed on day 7 post exposure with crocidolite, tremolite asbestos and erionite (Figure 2). Despite

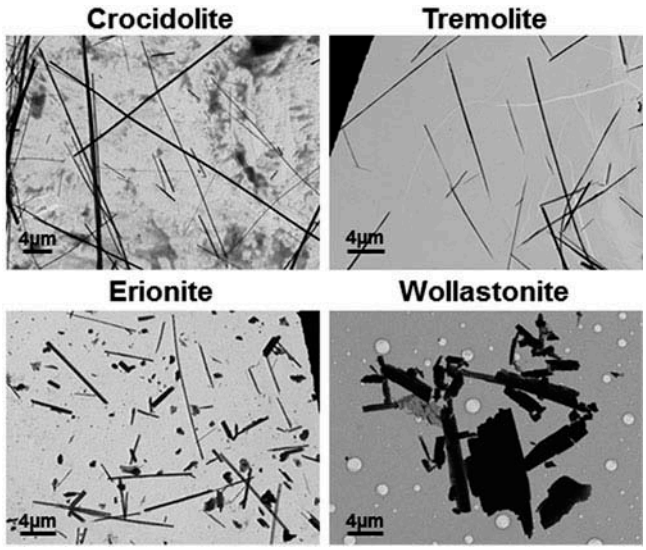

Figure 1. Representative TEM micrographs of different asbestos/asbestiform fibers . The different fibers studied include a zeolite fibrous material, erionite fibers from Rome, OR, two types of amphibole asbestos fibers (tremolite and crocidolite) and a low pathogenicity wollastonite fibers. The scale bar shown in the lower left corner of each image corresponds to 2 μm size.

Table 1. The Physical Dimensions of Various Mineral Fibers Estimated Using Transmission Electron Micrographs. A Minimum of Three Hundred Fibers per Sample ($N = 3$) Were Counted for Characterizing Each Fiber Type

	Erionite	Crocidolite	Tremolite	Wollastonite
Median length, μm	2.32	4.45	6.74	2.77
Length Range (Min-Max), μm	0.23–51.24	0.18–75.89	0.49–59.0	0.43–45.10
Median width, μm	0.20	0.13	0.16	0.82
Width Range (Min-Max), μm	0.01–1.01	0.02–0.64	0.03–0.96	0.13–5.80
Median Aspect ratio, μm	12.94	35.95	43.39	3.5
AR Range (Min-Max), μm	1.93–234.21	2.50–820.84	2.71–317.44	0.33–39.44

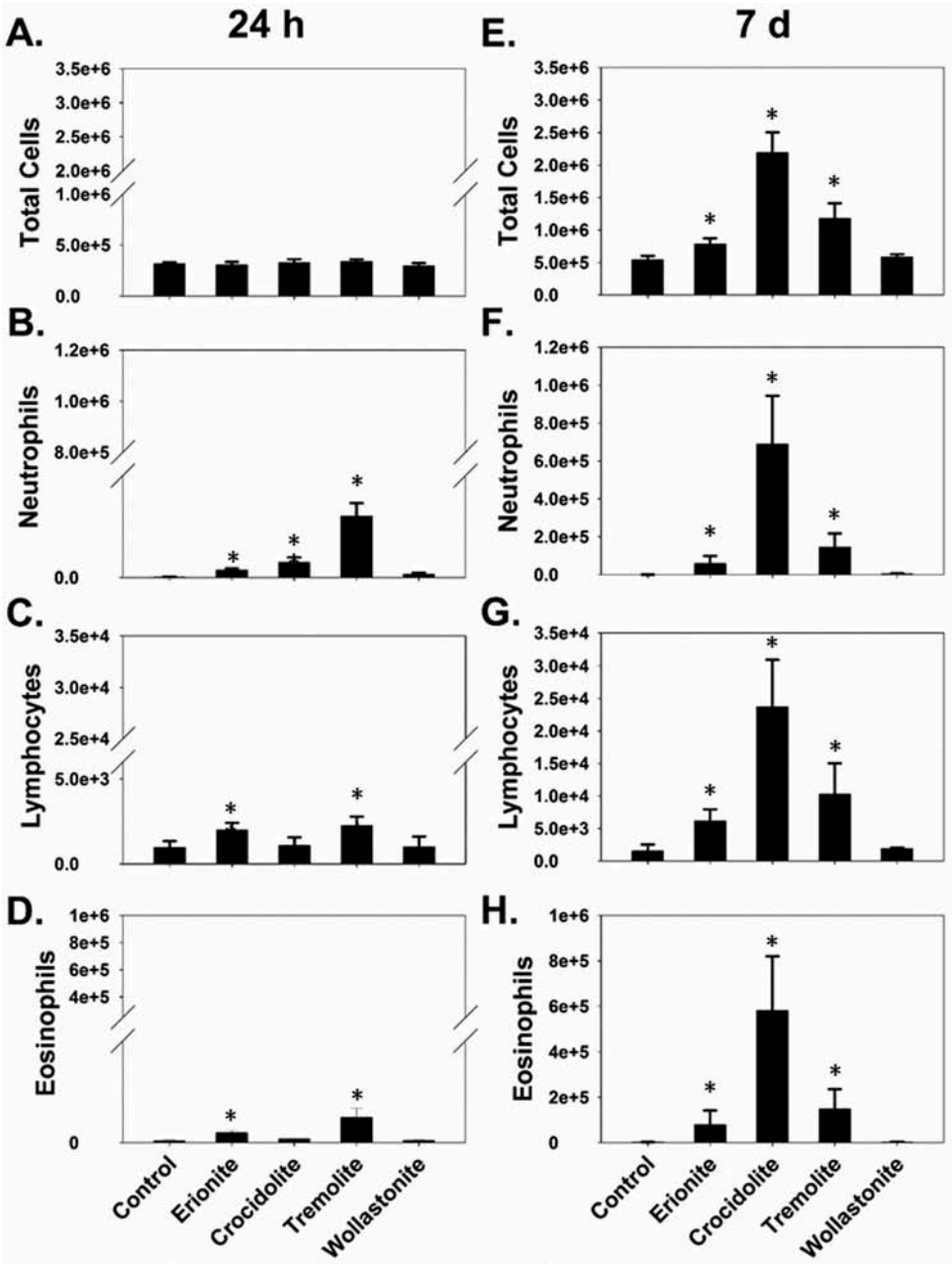

Figure 2. Cellular differentials in the broncheoalveolar lavage (BAL) fluid in mice Total cells and the accumulation of neutrophils, lymphocytes and eosinophils in BAL fluids of C57BL/6 mice 24 hr (A) and 7 days (B) after pharyngeal aspiration with different amphibole asbestos and erionite mineral fibers (80 μg/mouse). Mean + SEM (n = 5 mice/group). *$p < 0.05$ compared to control.

Downloaded by [Stephen B. Thacker CDC Library] at 09:00 11 January 2018

Downloaded by [Stephen B. Thacker CDC Library] at 09:00 11 January 2018

the lack of significant changes in total cells, BAL cytology indicated an increased accumulation of PMN on day 1 post exposure observed after pharyngeal aspiration with different asbestos and erionite mineral fibers. A significant increase in eosinophils and lymphocytes was observed 24 hr after aspiration exposure to erionite and tremolite asbestos fibers (Figure 2). These results indicate a differential inflammatory response with PMN influx peaking at day 1 and eosinophil response at day 7 post-treatment found for both erionite and tremolite asbestos. In contrast, exposure to crocidolite induced a "prolonged" inflammatory response with greater influx of neutrophils and eosinophils occurring on day 7 post exposure. The influx of both neutrophils and eosinophils—to a similar extent—dominated the inflammatory responses on day 7 post tremolite asbestos and crocidolite treatment, while a predominance of eosinophils was observed after erionite exposure (Figure 2).

Tissue damage response detected in BAL fluid

The degree of pulmonary damage was assessed by LDH activity in the BAL fluid recovered from mice 24 hr and 7 days post pharyngeal aspiration. LDH activity levels were significantly elevated on days 1 and 7 post exposure to crocidolite, tremolite asbestos and erionite fibers. More pronounced pulmonary damage was seen at day 7 post administration whereas

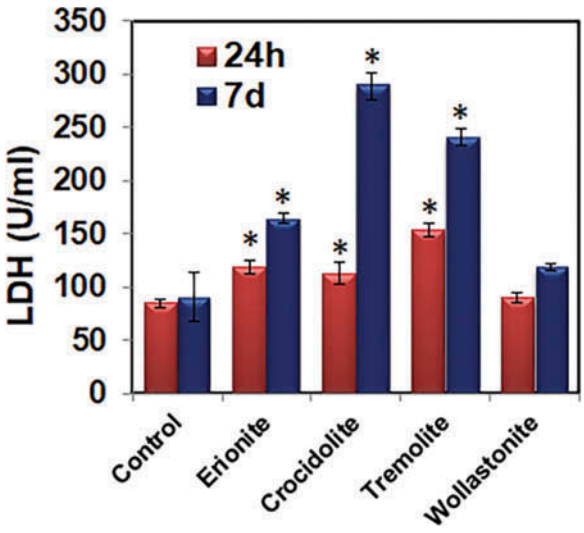

Figure 3. Tissue damage as evaluated by change in lactate dehydrogenase (LDH) activity Data presented in each case corresponds to actual LDH values (U/ml). *$p < 0.05$ compared to control (PBS) exposed mice. Means ± SE ($n = 5$ mice per group).

the magnitude of responses was higher for treatments with tremolite or crocidolite asbestos than erionite fibers (Figure 3, blue bars). This is also in agreement with a "prolonged" inflammatory response with maximal PMN influx at day 7 post crocidolite exposure and a sustained inflammatory response at 24 hr and day 7 post treatment to tremolite asbestos (Figure 2).

Accumulation of inflammatory mediators (cytokines/chemokines)

Cytokines and chemokines are important mediators of biological responses. Therefore, 23 different cytokines/chemokines were measured in the lungs at 24 hr (Table S1) and 7 days (Table S2) post exposure to erionite, tremolite asbestos, crocidolite and wollastonite particles. Of the four different fiber minerals tested, treatment with wollastonite indicated the overall least effect in inflammatory responses both after 24 hr and 7 days post exposure (Tables S1 & S2). The cytokines IL-5 and G-CSF at 24 hr and IL-4, IL-5, KC, IL-12p40 and MIP-1α at 7 days following administration of erionite, tremolite asbestos and crocidolite were found to be increased (Figure 4). At both time points investigated, the levels of Rantes were observed to be significantly elevated only after exposure to erionite and not to other materials investigated in this study (Table S1 & S2). In particular, the responses upon exposure to tremolite asbestos and crocidolite were more similar and significantly elevated secretion of pro-inflammatory cytokines such as IL-6, MCP-1, and KC at 24 hr (Figure 4A) and IL-6, G-CSF, MIP-1β and MCP-1 at 7 days post exposure (Figure 4B). While the expression of MIP-1α and MIP-1β was only found in tremolite asbestos exposed lungs at 24 hr, a significant rise in IL-1α, IL-1β and IL-13 concentrations was unique to crocidolite in lungs at 7 days (Figure 4B, Table S2).

Further the hierarchical cluster analysis was applied to highlight differences between various materials treatments at each time point. The dendrograms after 24 hr and 7 days post exposure are illustrated in Figure 4C and 4D, respectively. Both dendrograms demonstrate that the Euclidean distance between tremolite asbestos and crocidolite and other treatments is quite large. At both time points a close clustering of tremolite asbestos fibers to crocidolite was observed. Further, the dendrograms at 24 hr and 7 days seem to separate amphibole asbestos (i.e., tremolite and

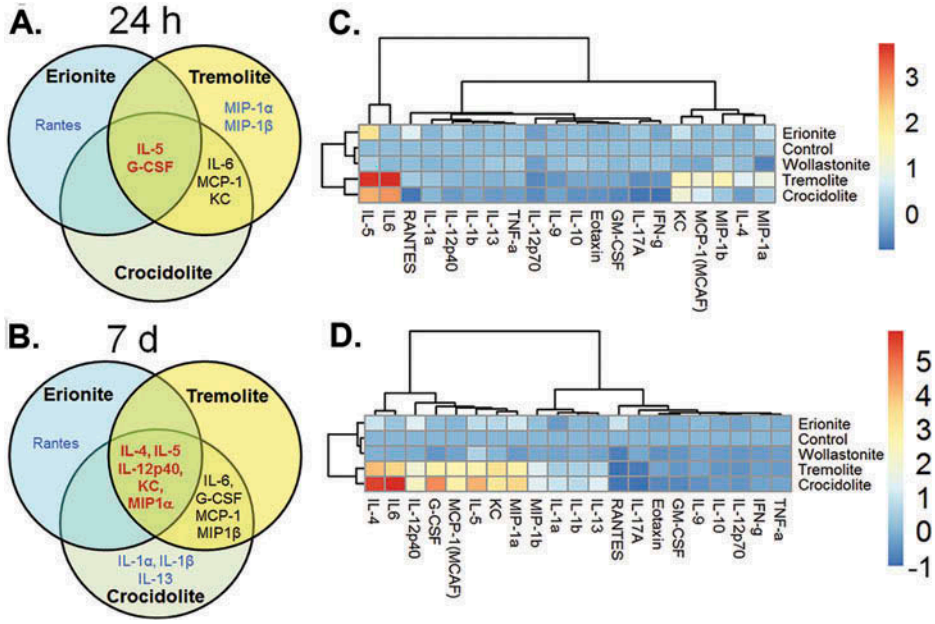

Figure 4. Differential responses in the inflammatory mediators after 24 hr and/or 7 days. Venn diagram comparing the changes in the cytokines/chemokines levels upon (A) 24 hr and (B) 7 day post exposure. The responses common to three types of fibers and unique to each are highlighted and colored in red and blue, respectively. Hierarchical clustering analysis of cytokine responses in the lungs at (C) 24 hr and (D) 7 day post exposure to different asbestos/asbestiform materials. The responses in cytokines/cytokines were clustered based upon Euclidean distance metric and complete linkage clustering method and the samples dendrogram was reordered based on their (dis-) similarities in cytokines responses, measured in the lungs at each post exposure time point. Each branch in the dendrogram shows similarity between samples, that is, the shorter the branch, the more similar.

crocidolite) from other treatments (Figure 4C–D). Data indicate that the average cytokine responses after tremolite asbestos administration were quite similar to those induced by crocidolite. The distance of wollastonite fiber samples, a known low-pathogenicity fiber, from the control group was less at both post exposure time points, suggesting a diminished inflammatory responses compared to other asbestos/asbestiform fiber materials investigated as part of this study. However, the distance of erionite fiber treatment from tremolite asbestos and crocidolite cluster and from that of control group was large at both post exposure time points, indicating that the mean cytokine responses after erionite exposure are quite different from other asbestos fibers materials examined (Figure 4C-4D).

Transcriptomics analysis and changes in gene expression

Analysis of the genes responding to different asbestos/asbestiform fiber treatments in the lungs at day 7 post exposure resulted in identification of a total of 78, 1716, 413 and 133 genes with a significant fold change ≥ ± 2.5 in erionite, crocidolite, tremolite asbestos or wollastonite samples, respectively (File S1). With the exception of wollastonite, the transcriptional regulation/response in lungs followed similar trends of inflammatory and pulmonary damage observations noted on day 7 post exposure to erionite, tremolite asbestos and crocidolite (Figure 2–3, 7 day). Detailed comparative analysis of all differentially expressed genes (DEG) revealed 31↑/47↓, 376↑/1340↓, 193↑/220↓ or 92↑/41↓ up (↑)/down (↓) regulated genes in response to erionite, crocidolite, tremolite asbestos or wollastonite exposures, respectively (Figure 5). Aspiration treatment with all four materials up-regulated 1 (Clca3) and down-regulated 3 (PER3, KLHL2, HLF) common genes. These common DEG were related to circadian rhythm/entrainment or ion channel transport pathways, or transcriptional activity processes (File S2). Compared to erionite and tremolite asbestos, exposure to crocidolite fibers resulted in the greatest number of DEG, albeit predominantly down-regulated genes (approximately 84%). This observation is consistent with "delayed" inflammatory and tissue damage responses occurring on day 7 post crocidolite treatment, in comparison to erionite and tremolite

Downloaded by [Stephen B. Thacker CDC Library] at 09:00 11 January 2018

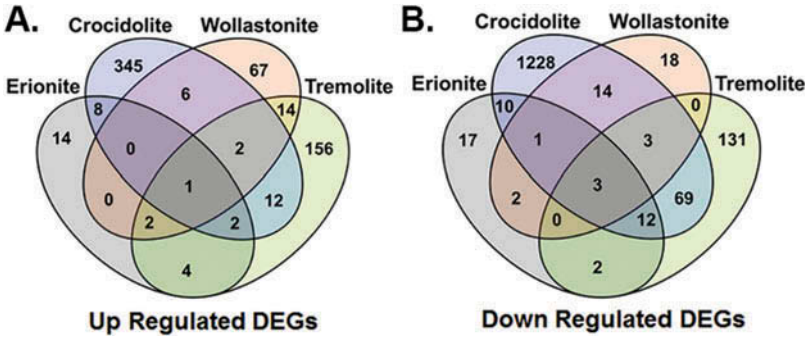

Figure 5. Total number of differentially regulated genes in the lungs at 7 days post exposure. Venn diagram showing differentially (A) up and (B) down regulated genes common and unique to various asbestos/asbestiform fiber treatments.

asbestos (Figures 2 and 3) or other fibrous nanomaterials (Murray et al. 2012). With the exception of wollastonite, exposure to the other three materials resulted in predominantly down-regulated DEG. However, upon administration of wollastonite most of the DEG were found to be up-regulated (approximately 70%). The top 10 most significantly up- and down-regulated genes upon different exposures are presented in Table 2. With the exception of chloride channel accessory 1 (CLCA1), none of the other top 10 significantly up- and down regulated genes overlapped between all four exposed groups. Overall, these results suggest that majority of genes modulated by treatment with tremolite responded similarly to crocidolite but not to erionite or wollastonite (Figure 5).

Pathways perturbed by various asbestos/ asbestiform fibers

To identify pathways that are altered in mice upon exposure to different asbestos/asbestiform fibers, pathway enrichment analysis was performed using Enrichr Pathways module for KEGG 2015. Pathways analysis of DEG at 7 days treatment to crocidolite, tremolite asbestos, erionite and wollastonite in mouse lungs predicted the significant involvement of a total of 39, 29, 11, and 6 pathways,

Table 2. The Top Ten Most up and down Regulated Genes upon Exposure to Asbestos/Asbestiform Fibrous Materials. The Text Highlighted in Bold Correspond to Genes that are Common to All Fiber Exposures

	GeneSymbol (FC)		
Crocidolite	Tremolite	Erionite	Wollastonite
Top 10 UP Regulated Genes			
A430060F13Rik (15.1)	MMP12 (21.7)	**CLCA1 (9.3)**	ADIPOQ (9.7)
B430212C06Rik (11.4)	Retnla (13.5)	Retnla (9.2)	Mup1 (8.8)
CLCA1 (10.9)	Sprr2a3 (10.5)	Gm3896 (5)	ALB (7.6)
Prl3b1 (10.9)	**CLCA1 (9.8)**	Speer4a (3.4)	CYP3A5 (5.8)
Defb10/Defb11 (9.4)	ALB (9.8)	SNORA69 (3.3)	SERPINA1 (5.4)
Aym1 (8.3)	Speer4a (9.3)	SNORD22 (3.3)	CHRNB3 (5.1)
MMP12 (8.1)	REG3G (8.2)	PRPF40B (3.2)	**CLCA1 (5)**
Nrg1 (7.5)	4930572O03Rik (8.1)	CUTA (3.2)	Igh (4.9)
ELN (7.1)	Ccl9 (7.3)	GABARAP (3.2)	ARNTL (4.3)
OARD1 (6.9)	Saa3 (7)	NT5C3B (3.1)	1700057H21Rik (4.3)
Top 10 DOWN Regulated Genes			
SNORD61 (-9.8)	CYP2F1 (-6.6)	TNS2 (-4)	SNORD61 (-3.3)
ATP8A1 (-8.1)	HPGD (-6.4)	ALB (-4)	KLHL2 (-3.2)
EPB41L4A (-7.5)	TNRC18 (-4.9)	CARMIL1 (-3.5)	CAPNS1 (-3.2)
SLC35A5 (-7.2)	Ppbp (-4.8)	POU2AF1 (-3.4)	RPS25 (-3.1)
SARNP (-6)	RAMP1 (-4.8)	HIST1H4D (-3.3)	NR1D1 (-3.1)
Gm4956 (-5.8)	Gm6358 (-4.6)	Ms4a4b (-3.2)	SLC38A10 (-3.1)
TNS2 (-5.7)	Gm8541 (-4.4)	PER2 (-3.1)	HLF (-3)
Ms4a4b (-5.7)	Gm13301 (-4.4)	CUL2 (3)	RSPH4A (-3)
CSGALNACT2 (-5.7)	C330024D21Rik (-4.3)	PPP1R16B (2.9)	Sik1 (-2.9)
API5 (-5.6)	CLEC1A (-4)	CAPNS1 (2.9)	P4HA2 (-2.9)

Downloaded by [Stephen B. Thacker CDC Library] at 09:00 11 January 2018

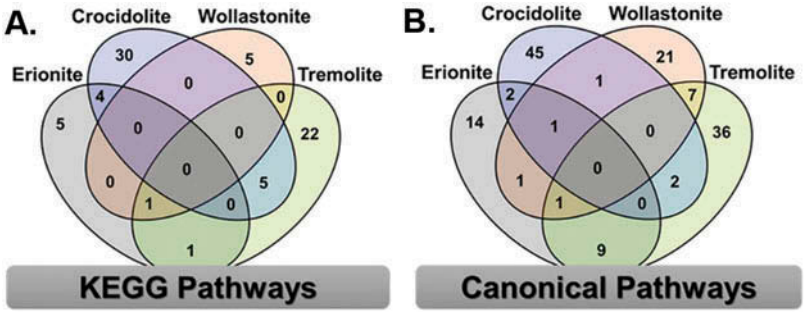

Figure 6. Enrichment analysis of pathways associated with dysregulated genes in the lungs of erionite, crocidolite, tremolite asbestos and wollastonite exposed mice. Venn diagrams showing common and unique enriched (A) KEGG signaling pathways and (B) canonical pathways from IPA.

Downloaded by [Stephen B. Thacker CDC Library] at 09:00 11 January 2018

respectively (Figure 6A). None of the pathways were common to all material exposure. With the exception of crocidolite, enrichment of "circadian rhythm" pathway was found to be common to the other three particle treatments (File S2). Pathways associated with the immune system such as leukocyte transendothelial migration, complement and coagulation cascades and toll-like receptor signaling as well as stress and injury including cytokine-cytokine receptor interactions and ECM-receptor interactions, were uniquely represented by up-regulated genes upon tremolite asbestos administration. Most importantly, several pathways related to cancer including pathways in cancer and non-small cell lung cancer, signal transduction pathways such as vascular endothelial growth factor (VEGF), and cellular processes such as apoptosis, adherens junction and tight-junction signaling were uniquely enriched by down-regulated genes upon crocidolite exposure. The "transcriptional misregulation in cancer" pathway was commonly enriched upon treatment with either crocidolite or erionite.

IPA core analysis of DEG at 7 days exposure to crocidolite, tremolite asbestos, erionite or wollastonite in mouse lungs predicted the involvement of a total of 51, 55, 28, and 32 enriched canonical pathways, respectively (Figure 6B) and are presented in File S3. The top canonical pathways associated with DEG on day 7 post-treatment with erionite, crocidolite, tremolite asbestos and wollastonite included adipogenesis pathway, epithelial adherens junction signaling, LXR/RXR activation and circadian rhythm signaling, respectively. While altered inflammatory pathways such as acute phase response signaling, clathrin-mediated endocytosis signaling, LXR/RXR and FXR/RXR signaling were observed to be commonly enriched at day 7 post exposure to tremolite asbestos or wollastonite fibers, B-cell receptor signaling and apoptosis signaling were commonly perturbed upon administration of crocidolite or erionite. The circadian rhythm signaling pathway was predicted to be commonly perturbed among tremolite asbestos, erionite and wollastonite exposures. In addition, phosphatase and tensin homolog (PTEN), nuclear factor kappa-B (NF-kB) activation and apoptosis signaling pathways were predicted to be activated upon exposure to crocidolite. Several pathways related to cellular processes such as transforming growth factor-beta (TGFb-), VEGF-, platelet derived growth factor (PDGF-), interleukin 8 (IL8-) and chemokine signaling were predicted to be down-regulated in the lungs treated with crocidolite. A predicted activation of mostly canonical pathways related to inflammation including acute phase response, toll-like receptor, p38 mitogen activated protein kinase (p38 MAPK), NF-kB and Interleukin 6 (IL6) signaling was found upon administration of tremolite asbestos (File S3). Similarly, exposure to wollastonite resulted in the predicted activation of pathways related to inflammation including acute phase response signaling and oxidative stress such as production of nitric oxide and reactive oxygen species in macrophages. Importantly, the DEG that participate in signaling pathways, including apoptosis, circadian rhythm/entrainment and disease pathways related to cancer/systemic responses, were previously reported (Nymark

Downloaded by [Stephen B. Thacker CDC Library] at 09:00 11 January 2018

et al. 2007; Roe et al. 2009) to be activated upon exposure to asbestos materials (File S2 & S3).

Gene signaling network analysis

The IPA top-ranked gene signaling networks (GSN) were examined to identify potential networks and mechanisms perturbed upon fiber exposures. The top 10 gene networks predicted using IPA, along with significance scores, with number of DEG involved in each network, are listed as Supplemental material, File S5. The top-ranked signaling networks at 7 days post-treatment was as follows: (1) crocidolite was "Cell Death and Survival, Tissue Morphology, Hematological System Development and Function" (score: 35); (2) tremolite asbestos was "Cellular Movement, Immune Cell Trafficking, Cellular Function and Maintenance" (score:51); (3) erionite was "Cellular Development, Cellular Growth and Proliferation, Hematological System Development and Function" (score:20) and (4) wollastonite was "Hematological System Development and Function, Tissue Morphology, Cell-To-Cell Signaling and Interaction" (score: 21). In the case of crocidolite, in addition to the top GSN, the second and third most significant GSN also displayed similar scores. The molecules in the top ranked GSN were predominantly involved in "molecular mechanisms of cancer" and "IL-8/VEGF/NF-kB/P53" signaling in the case of crocidolite exposure. For tremolite asbestos it was "granulocyte/agranulocyte adhesion and diapedesis", "Rheumatoid Arthritis signaling", "P38 MAPK signaling" and "communication of innate and adaptive immune cells"; In the case of erionite it was " glucocorticoid receptor signaling" and "rheumatoid arthritis signaling". Finally for wollastonite it was in the "production of nitric oxide and reactive oxygen species in macrophages" and "IL-12 signaling and production in macropahges" (File S5, Charts). Overall, these results suggest significant differences in biological responses exerted by different asbestos/asbestiform fibers, involving unique cellular regulatory processes. This is further supported by the hub genes in the top-ranked GSN and genes that are unique to each exposure (File S5, Highlighted in bold).

Histological alterations

The lungs were stained with hematoxylin and eosin (H&E) and trichrome and quantitatively assessed for histopathologic abnormalities, including abnormalities of the parenchymal architecture (bronchioles, alveoli, pleura, and vasculature), abnormal inflammatory infiltrates, presence or absence of acute lung injury, and presence or absence of fibrosis. Microscopic analysis of lungs from controls revealed normal histology of conductive and respiratory airways at 7 and 56 days (Figure 7; Table 3). Seven days after exposure to erionite, sections reveal mild acute peribronchial and parenchymal inflammatory infiltrate, composed predominantly of neutrophils. There was no significant bronchial hyperplasia or endobronchial inflammation. Seven days after crocidolite or tremolite asbestos administration moderate

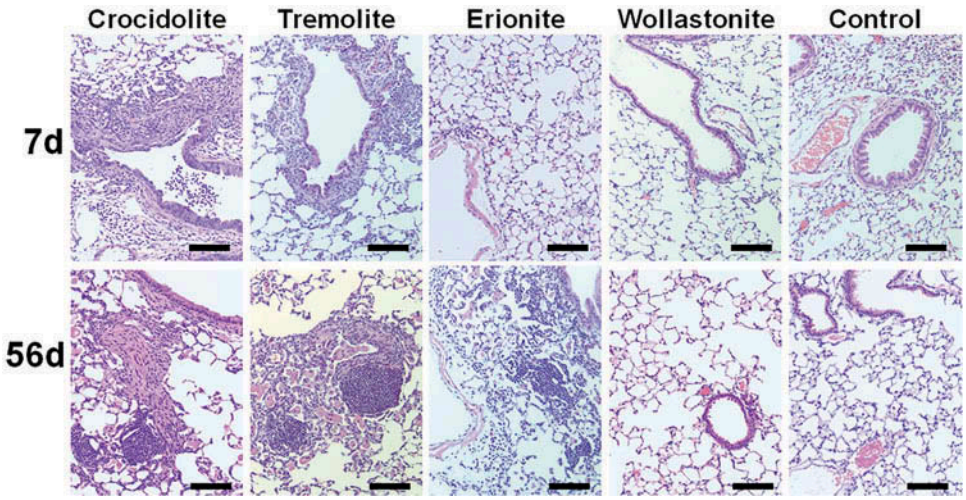

Figure 7. Pathological examination of lung tissue from C57BL6 mice at day 7 and 56 post exposure. The lung sections stained with hematoxylin and eosin (H&E, x200), were used for histopathologic evaluations. The scale bar corresponds to 100 μm.

Downloaded by [Stephen B. Thacker CDC Library] at 09:00 11 January 2018

Table 3. Pathologic Alterations at 7 and 56 Days Post Exposure to Erionite, Crocidolite, Tremolite and Wollastonite. Hyperplasia and Inflammation are Assessed on H&E Stain; Fibrosis Was Assessed on Trichrome Stained Slides. Pathologic Grading Corresponds to as Follows: 0 – Negative, 1 – Mild, 2 – Moderate, 3 – Severe

	Bronchoepithelial Hyperplasia		Endobronchial inflammation		Peribronchial inflammation		Perivascular inflammation		Parenchymal inflammation		Granulomas		Fibrosis	
Time	7d	56d	7d	56d	7d	56d	7d	56d	7d	56d	7d	56d	7d	56d
Control	0	0	0	0	0	0	0	0	0	0	0	0	0	0
	0	0	0	0	0	0	0	0	0	0	0	0	0	0
	0	0	0	0	0	0	0	0	0	0	0	0	0	0
	0	0	0	0	0	0	0	1	0	0	0	0	0	0
	0	0	0	0	0	0	0	0	0	0	0	0	0	0
Erionite	1	0	1	0	2	0	0	1	1	1	0	0	0	0
	0	0	0	0	0	1	0	1	0	1	0	0	0	1
	0	0	0	0	1	0	1	1	0	0	0	0	0	1
	0	0	0	0	1	1	0	1	0	2	0	0	0	0
	1	1	0	1	1	0	0	1	1	1	0	0	0	2
Crocidolite	2	1	2	1	2	3	1	3	2	3	1	3	0	3
	1	1	2	1	2	3	1	3	2	2	3	3	0	2
	1	1	2	1	2	3	1	3	2	3	2	3	0	2
	1	1	2	2	2	3	1	3	2	3	2	3	0	2
	3	1	2	1	2	3	1	3	2	3	3	3	0	2
Tremolite	2	1	2	1	2	2	1	2	2	3	2	3	0	2
	1	1	2	1	2	1	0	1	1	1	1	2	0	1
	2	1	2	1	2	1	0	1	1	1	2	1	0	1
	1	2	2	1	2	3	1	3	2	3	1	3	1	2
	1	1	2	1	2	2	1	2	2	3	3	3	1	2
Wollastonite	0	0	0	0	0	0	0	0	0	0	0	0	0	1
	0	0	0	0	0	0	0	0	0	0	0	0	0	0
	0	1	0	0	0	0	0	0	0	0	0	0	0	1
	0	0	0	0	0	1	0	1	0	0	0	0	0	1
	0	0	0	0	0	1	0	1	0	0	0	0	0	0

Downloaded by [Stephen B. Thacker CDC Library] at 09:00 11 January 2018

acute and chronic endobronchial and peribronchial inflammation and bronchial hyperplasia was observed. A moderate to severe parenchymal inflammation with numerous epithelioid granulomata along with mild perivascular chronic inflammation was also detected but without evidence of fibrosis (Figure 7). Fifty-six days after exposure to erionite, mild chronic peribronchial and perivascular inflammation were noted along with mild to moderate parenchymal lymphocytic infiltration and fibrosis. No granulomata were detected (Figure 7, 56 day). Fifty-six days after administration of crocidolite or tremolite asbestos microscopy revealed mild chronic endobronchial inflammation and epithelial hyperplasia. Exposure to crocidolite induced severe peribronchial, perivascular and parenchymal inflammation with numerous epithelioid granulomata. There was also moderate to severe peribronchial and perivascular fibrosis. (Figure 7). Similar pattern of inflammation and fibrosis was seen in tremolite asbestos group, but alterations were less prominent (moderate) (Figure 7). Exposure to wollastonite did not induce detectable inflammation, hyperplasia or fibrosis at day 7. (Figure 7). At 56 days, there were no significant peribronchial or parenchymal inflammation, but in some cases there was mild perivascular inflammation and fibrosis. Overall, the severity of the histological alterations found in this study was in the order: crocidolite ≥ tremolite asbestos > erionite > wollastonite (Table 3).

Discussion

In the present study, global gene expression profiles and pulmonary toxicity were evaluated in mice at day 7 post pharyngeal aspiration exposure to 3 types of asbestos and/or asbestiform fibers erionite, crocidolite, tremolite asbestos and a low pathogenecity mineral fiber, wollastonite. Changes in pulmonary gene expression profiles upon various asbestos/asbestiform fiber treatment were identified and compared with each other. Further, the identified genes and pathways perturbed upon fiber administration were consistent with the corresponding pulmonary pathological and biochemical outcomes.

Biological responses to airborne particulates are orchestrated by release of a number of inflammatory mediators. It was found that majority of cytokines/chemokines including IL-4, IL-5, IL-12p40, KC, and MIP-1α were up-regulated upon aspiration exposure to all three pathogenic materials—crocidolite, tremolite asbestos, and erionite fibers (Figure 4B). Increased release of cytokines/chemokines is consistent with the recruitment of phagocytic cells including eosinophils, neutrophils, and monocytes/macrophages (Figure 2). While accumulation of IL-6, G-CSF, MIP1-β and MCP-1 were common to tremolite asbestos and crocidolite exposure, up-regulation of Rantes was seen only after treatment with erionite fibers (Figure 4). The marked rise in IL-1α and IL-1β upon crocidolite and MCP-1 upon crocidolite and tremolite asbestos treatment is further supported by an increased accumulation of macrophages, and PMN, key producers of pro-inflammatory cytokines (Figure 2). The overexpression of IL-5 is compatible with elevated number of eosinophils and an important role of this cytokine is in eosinophil growth and differentiation (Clutterbuck, Hirst, and Sanderson 1989; Zabeau et al. 2003). Similarly, the overall increased IL-5 levels at day 7 post exposure to crocidolite (Figure 2) are in agreement with elevated general accumulation of eosinophils, compared to other fiber exposures (Figure 4;Table S2). Moreover, Rantes, a chemokine upregulated only upon erionite exposure, is known to be overexpressed in many cancers and plays important roles in proliferation, invasion of cancer cells, and angiogenesis (Aldinucci and Colombatti 2014). Further, enhanced expression of this gene in malignant mesothelioma (MM) cells *in vitro* as well as its secretion in pleural fluid of MM tumor-bearing mice was reported previously (Hillegass et al. 2010; Shukla et al. 2013). This may account for the observed increased incidence of MM in humans and mice exposed to erionite (Carbone et al. 2011; Carbone and Yang 2012; Wagner et al. 1985). Taken together, data suggest that inflammatory and cytokine responses might precede and be critical for development of the carcinogenic outcomes such as MM or lung cancer observed upon exposure to different asbestos/asbestostiform fibers. These findings also suggest that erionite mineral fibers, regardless of having the same shape and size as amphibole asbestos fibers, may induce differing biological responses.

Downloaded by [Stephen B. Thacker CDC Library] at 09:00 11 January 2018

Significant differences in the magnitude of various pathological alterations were observed upon exposure to various asbestos/asbestiform fibers. Administration of wollastonite induced significantly less inflammation and fibrosis in lungs compared to erionite, crocidolite or tremolite asbestos (Figure 6 and S3). Previous studies reported that fiber length and higher aspect ratio might correlate directly with fibrosis severity of different amphibole asbestos materials (Boulanger et al. 2014; Cyphert et al. 2012). Thus a low biological response to wollastonite, possessing the smallest aspect ratio compared to other materials investigated, is not entirely unexpected and consistent with previous observations (Cambelova and Juck 1994 ; Governa et al. 1998). In contrast, despite displaying similar fiber sizes as crocidolite and tremolite asbestos, exposure to erionite also induced consistently less pathological responses with no granulomatous lesions in the lungs (Figure 6 and S3). Epithelial cell injury, due to increased reactive oxygen species (ROS) production is generally regarded as a crucial step in the onset of fibrotic pulmonary conditions (Aljandali et al. 2001; Tatrai et al. 2005). Elevated numbers of activated inflammatory cells with their potent ROS-generating machinery may be the major contributors to the production of injurious ROS. Notably, transition metals, particularly iron (Fe), may also play a catalytic role in redox-cycling activity of ROS thus enhancing overall oxidative damage (Fach et al. 2003; Ghio 2009). It has been shown that both crocidolite and erionite exhibit their toxicity, at least in part, through the formation of $HO^{\bullet}$ radicals in Fenton reaction (Fach et al. 2003; Ghio et al. 2009; Goodglick and Kane 1986; Mossman and Marsh 1989; Shatos et al. 1987). As recent studies indicate that these fibers' amorphization and dissolution rate in tissues are very slow compared to chrysotile, requiring decades, not days, this has been interpreted in a way, that Fe-mediated potential toxicity may be relatively low (Gualtieri et al. 2017; Pollastri et al. 2016). In our study, the cytokines and other responses were assessed 7 days post exposure, while several other investigators only detected significant amounts of Fe in mouse lungs after one month post-treatment (Ghio et al. 2009; Pascolo et al. 2016; Trevisan et al. 2016). However, Fe does not need to be released in the free form to participate in the redox cycling reactions. Thus, Fe-related redox activity may contribute to alterations in redox-environment and overall toxicity. Direct EPR assessments of Fe-driven redox reactions may be useful in specifying the role of this mechanism. Alternatively, direct aspect ratio dependent mechanical effects of the fibers are known to contribute to the fibrous particles toxicity (Donaldson et al. 1993; Pinkerton et al. 1990; Tatrai et al. 2005). Data suggest that, in addition to length, fiber characteristics such as number, mineral composition, aspect ratio and/or other factors might be responsible for decreased biological responses upon erionite and/or wollastonite administration noted in this study. It was observed that the total number of fibers for erionite or wollastonite was comparatively less to that of crocidolite or tremolite asbestos materials (Figure 1). This possibility is further supported by previous findings that reported lower biological responses to erionite than those to asbestos fibers when compared on an equal mass basis (Brown, Davies, and Rood 1989; Palekar et al. 1987; Palekar, Most, and Coffin 1988).

Biological interactions of asbestos materials within body environment are able to switch cellular machinery through growth factors, inflammatory mediators and other receptor ligands to up and/or down regulate multiple signaling pathways thus leading to abnormal growth of the exposed cells (Churg 1996; Mossman and Churg 1998; Ramos-Nino, Timblin, and Mossman 2002). In this study, DEG in the top ranked GSN of IPA analysis upon exposure to crocidolite and tremolite asbestos fibers were associated with biological functions involved in cellular movement, cell death and survival, and cellular growth and proliferation (File S5). The recruitment of inflammatory cells (Quinlan et al. 1995; Rola-Pleszczynski, Gouin, and Begin 1984) and development of chronic inflammation is critical for cellular transformation processes both benign and malignant (Hillegass et al. 2010; Kamp, Shacter, and Weitzman 2011). Increased inflammatory responses and significant accumulation of macrophages and PMN was noted following crocidolite or tremolite asbestos administration (Figure 2). The enrichment analysis of DEG upon exposure

Downloaded by [Stephen B. Thacker CDC Library] at 09:00 11 January 2018

to crocidolite or tremolite asbestos revealed "lung cancer" and "pulmonary fibrosis" as the top two datasets with similar disease gene expression patterns (File S4). This is consistent with the incidence of granulomatous lesions and increased fibrosis observed upon exposure to amphibole asbestos fibers (Boulanger et al. 2014; Gavett et al. 2016). Enhanced expression of T_H2 inflammatory cytokines in BAL fluid such as IL-4, IL-5, IL-6, MIP1β, and MCP-1, known to play a key role in fibrosis (Emad and Emad 2007; Gasse et al. 2007; Mastruzzo, Crimi, and Vancheri 2002; Ogushi 1996; Wynn 2008; Zhang and Phan 1996), were found in mice treated with amphibole asbestos fibers such as crocidolite or tremolite (Figure 3). Moreover, elevated levels of IL-13, an IL-4-like cytokine secreted by activated T_H2 cells (Zurawski and De Vries 1994), were detected only in mice exposed to crocidolite fibers. In fact, increased levels of both IL-4 and IL-13 are known to play an important role in fibrotic diseases (Doucet et al. 1998; Gharaee-Kermani et al. 2001; Zhu et al. 1999). This is consistent with enhanced pulmonary fibrotic responses observed in mice at day 56 post exposure to crocidolite compared to other fibers (Figure 4; Table 3).

Another notable finding in this study was the up-regulation of genes including CULA, GABARAP and ALDH1A3 in the lungs exposed to erionite with expression similar to "malignant mesothelioma of pleura" (File S4), despite the lack of severe fibrotic responses and no apparent granuloma formation (Figure 7). Erionite mineral fibers are known to trigger mesothelioma in rodents and humans as well as possessing a higher intrinsic transformation ability than other amphibole asbestos fibers (Carbone et al. 2011; Carbone and Yang 2012; Wagner et al. 1985). While the biological responses as a consequence of exposure to erionite are less pathogenic than crocidolite and tremolite asbestos, several genes were found to be uniquely regulated upon erionite administration. Some of these genes were previously reported to play key role in epithelial cancer including FGF2, CAMKV, ALDH1A3, PPP1R3G, and PDK1), invasion of epithelial tissue such as FGF2, TCF3, and ALDH1A3 as well as cell death. Further, both erionite and tremolite asbestos were reported to induce T_H17 responses and exert a role in autoimmune diseases including rheumatoid arthritis (Noonan et al. 2006; Pfau, Serve, and Noonan 2014). Consistent with this, the DEG in the top-ranked GSN, upon treatment with erionite or tremolite asbestos were found to be involved in "Rheumatoid Arthritis signaling" (File S5, Erionite_Down_DEGs). While microarray analysis indicated signaling pathways and mechanisms that might suggest that erionite fibers exhibit the ability to induce pathogenic/carcinogenic responses in mice, histopathological sections did not show any such manifestations. A possible explanation for the lack of granulomatous lesions and decreased pathological responses in mice exposed to erionite may simply reflect that more time is needed for development of pathology, thus requiring longer duration studies. Another possibility might be that the overall smaller lengths of erionite compared to other amphiboles may have resulted in efficient clearance from lungs (Figure 1; Table 1). This observation is consistent with a recent study that reported erionite fibers, because of their smaller size, compared to crocidolite and other asbestos fibers were successfully phagocytosed by cells (Gandolfi et al. 2016). Frustrated phagocytosis of long fibers (longer than ~15 μm in length (Poland et al. 2008)) by macrophages is a determining factor in initiating granuloma formation (Donaldson et al. 2010; Searl et al. 1999).

Conclusions

In conclusion, a comprehensive assessment of pulmonary responses was performed following exposure to 4 types of asbestos/asbestiform fibers. The results presented suggest that the underlying mechanisms leading to asbestos/asbestiform fiber-induced carcinogenic outcomes may vary. Data demonstrated that both amphibole asbestos and erionite mineral fibers elicited tissue damage and increased inflammatory responses; however, the extent of these responses varied significantly depending upon the type of fibrous material investigated. Specifically, of the four different types of materials examined, crocidolite followed by tremolite asbestos fibers, at an equal mass concentration, were deemed more pathologically active compared to other types. Overall, data reported here provide insights into

differing underlying mechanisms of non-carcinogenic and carcinogenic outcomes after exposure to amphibole asbestos versus asbestiform mineral fibers (e.g., erionite). Further detailed mechanistic long duration studies focusing on pulmonary outcomes and those correcting for identical fiber numbers and size distributions of various asbestos/asbestiform fibers are warranted, as the persistence of long fibers (>15 μm) and some of the inflammatory signatures, found in this study, indicate different chronic effects upon exposure to erionite mineral and other amphibole asbestos fibers. Such studies may also provide an opportunity to uncover the time dependent cellular and molecular changes as well as biological mechanisms associated with different asbestos/asbestiform fiber-mediated carcinogenesis.

Acknowledgments

The authors would like to thank Mariana Farcas (NIOSH) for her technical assistance during samples collection and processing.

Declaration of interests

The authors declare that they have no competing interests.

Disclaimer

The findings and conclusions in this report are those of the authors and do not necessarily represent the views of the National Institute for Occupational Safety and Health.

Funding

This work was supported by NORA 939051G.

References

Albrecht, C., P. J. Borm, and K. Unfried. 2004. Signal transduction pathways relevant for neoplastic effects of fibrous and non-fibrous particles. *Mutat. Res.* 553:23–35.

Aldinucci, D., and A. Colombatti. 2014. The inflammatory chemokine ccl5 and cancer progression. *Mediat. Inflamm.* 2014:292376.

Aljandali, A., H. Pollack, A. Yeldandi, Y. Li, S. A. Weitzman, and D. W. Kamp. 2001. Asbestos causes apoptosis in alveolar epithelial cells: Role of iron-induced free radicals. *J. Lab. Clin. Med.* 137:330–339.

Andujar, P., A. Lacourt, P. Brochard, J. C. Pairon, M. C. Jaurand, and D. Jean. 2016. Five years update on relationships between malignant pleural mesothelioma and exposure to asbestos and other elongated mineral particles. *J. Toxicol. Environ. Health. B* 19:151–172.

Bernstein, D., V. Castranova, K. Donaldson, B. Fubini, J. Hadley, T. Hesterberg, A. Kane, D. Lai, E. E. McConnell, H. Muhle, G. Oberdorster, S. Olin, and D. B. Warheit; IlSI Risk Science Institute Working Group. 2005. Testing of fibrous particles: Short-term assays and strategies. *Inhal. Toxicol.* 17:497–537.

Boulanger, G., P. Andujar, J. C. Pairon, M. A. Billon-Galland, C. Dion, P. Dumortier, P. Brochard, A. Sobaszek, P. Bartsch, C. Paris, and M. C. Jaurand. 2014. Quantification of short and long asbestos fibers to assess asbestos exposure: A review of fiber size toxicity. *Environ. Health* 13:59.

Brazma, A., P. Hingamp, J. Quackenbush, G. Sherlock, P. Spellman, C. Stoeckert, J. Aach, W. Ansorge, C. A. Ball, H. C. Causton, T. Gaasterland, P. Glenisson, F. C. Holstege, I. F. Kim, V. Markowitz, J. C. Matese, H. Parkinson, A. Robinson, U. Sarkans, S. Schulze-Kremer, J. Stewart, R. Taylor, J. Vilo, and M. Vingron. 2001. Minimum information about a microarray experiment (miame)-toward standards for microarray data. *Nat. Genet.* 29:365–371.

Brown, R. C., R. Davies, and A. P. Rood. 1989. Modification of fibrous Oregon erionite and its effects on in vitro activity. *IARC Sci. Publ.* 90:74–80.

Cambelova, M., and A. Juck. 1994. Fibrogenic effect of wollastonite compared with asbestos dust and dusts containing quartz. *Occup Environ Med* 51:343–346.

Carbone, M., Y. I. Baris, P. Bertino, B. Brass, S. Comertpay, A. U. Dogan, G. Gaudino, S. Jube, S. Kanodia, C. R. Partridge, H. I. Pass, Z. S. Rivera, I. Steele, M. Tuncer, S. Way, H. Yang, and A. Miller. 2011. Erionite exposure in North Dakota and Turkish villages with mesothelioma. *Proc. Natl. Acad. Sci. USA* 108:13618–13623.

Carbone, M., R. A. Kratzke, and J. R. Testa. 2002. The pathogenesis of mesothelioma. *Semin. Oncol.* 29:2–17.

Carbone, M., H. I. Pass, P. Rizzo, M. Marinetti, M. Di Muzio, D. J. Mew, A. S. Levine, and A. Procopio. 1994. Simian virus 40-like DNA sequences in human pleural mesothelioma. *Oncogene* 9:1781–1790.

Carbone, M., and H. Yang. 2012. Molecular pathways: Targeting mechanisms of asbestos and erionite carcinogenesis in mesothelioma. *Clin. Cancer Res.* 18:598–604.

Churg, A. 1996. The uptake of mineral particles by pulmonary epithelial cells. *Am. J. Respir. Crit. Care Med.* 154:1124–1140.

Clutterbuck, E. J., E. M. Hirst, and C. J. Sanderson. 1989. Human interleukin-5 (IL-5) regulates the production of eosinophils in human bone marrow cultures: Comparison and interaction with IL-1, IL-3, IL-6, and GMCSF. *Blood* 73:1504–1512.

Comar, M., N. Zanotta, G. Pesel, P. Visconti, I. Maestri, R. Rinaldi, S. Crovella, M. Cortale, R. De Zotti, and M. Bovenzi. 2012. Asbestos and SV40 in malignant pleural

Downloaded by [Stephen B. Thacker CDC Library] at 09:00 11 January 2018

Downloaded by [Stephen B. Thacker CDC Library] at 09:00 11 January 2018

mesothelioma from a hyperendemic area of north-eastern Italy. *Tumori* 98:210–214.

Cyphert, J. M., M. A. McGee, A. Nyska, M. C. Schladweiler, U. P. Kodavanti, and S. H. Gavett. 2016. Long-term toxicity of naturally occurring asbestos in male Fischer 344 rats. *J. Toxicol. Environ. Health A* 79:49–60.

Cyphert, J. M., A. Nyska, R. K. Mahoney, M. C. Schladweiler, U. P. Kodavanti, and S. H. Gavett. 2012. Sumas mountain chrysotile induces greater lung fibrosis in Fischer344 rats than Libby amphibole, El Dorado tremolite, and Ontario ferroactinolite. *Toxicol. Sci.* 130:405–415.

Dodson, R. F. 2016. Preface: Respirable elongated mineral particles and human health-revisited. *J. Toxicol. Environ. Health B* 19:149–150.

Dogan, A. U., Y. I. Baris, M. Dogan, S. Emri, I. Steele, A. G. Elmishad, and M. Carbone. 2006. Genetic predisposition to fiber carcinogenesis causes a mesothelioma epidemic in Turkey. *Cancer Res.* 66:5063–5068.

Donaldson, K., B. G. Miller, E. Sara, J. Slight, and R. C. Brown. 1993. Asbestos fibre length-dependent detachment injury to alveolar epithelial cells in vitro: Role of a fibronectin-binding receptor. *Int. J. Exp. Pathol.* 74:243–250.

Donaldson, K., F. A. Murphy, R. Duffin, and C. A. Poland. 2010. Asbestos, carbon nanotubes and the pleural mesothelium: A review of the hypothesis regarding the role of long fibre retention in the parietal pleura, inflammation and mesothelioma. *Part Fibre Toxicol.* 7:5–5.

Doucet, C., D. Brouty-Boye, C. Pottin-Clemenceau, G. W. Canonica, C. Jasmin, and B. Azzarone. 1998. Interleukin (IL) 4 and IL-13 act on human lung fibroblasts. Implication in asthma. *J. Clin. Invest.* 101:2129–2139.

Emad, A., and V. Emad. 2007. Elevated levels of MCP-1, MIP-alpha and MIP-1 beta in the bronchoalveolar lavage (BAL) fluid of patients with mustard gas-induced pulmonary fibrosis. *Toxicology* 240:60–69.

Everitt, B. S., S. Landau, M. Leese, and D. Stahl. 2011. Hierarchical clustering. In David, J. Balding, Noel, A.C. Cressie, Garrett, M. Fitzmaurice, Harvey Goldstein, Geert Molenberghs, David, W. Scott, Adrian F.M.Smith, Ruey S. Tsay, Sanford Weisberg (eds.). *Cluster analysis*, 71–110. John Wiley & Sons, Ltd. https://pdfs.semanticscholar.org/b05a/ca28ced3751d6302d8ce7396f80c90d612fd.pdf

Fach, E., R. Kristovich, J. F. Long, W. J. Waldman, P. K. Dutta, and M. V. Williams. 2003. The effect of iron on the biological activities of erionite and mordenite. *Environ. Int.* 29:451–458.

Frost, G., A. Darnton, and A. H. Harding. 2011. The effect of smoking on the risk of lung cancer mortality for asbestos workers in great britain (1971-2005). *Ann. Occup. Hyg.* 55:239–247.

Fubini, B., and I. Fenoglio. 2007. Toxic potential of mineral dusts. *Elements* 3:407.

Gandolfi, N. B., A. F. Gualtieri, S. Pollastri, E. Tibaldi, and F. Belpoggi. 2016. Assessment of asbestos body formation by high resolution feg-sem after exposure of Sprague-Dawley rats to chrysotile, crocidolite, or erionite. *J. Hazard. Mater.* 306:95–104.

Gasse, P., C. Mary, I. Guenon, N. Noulin, S. Charron, S. Schnyder-Candrian, B. Schnyder, S. Akira, V. F. Quesniaux, V. Lagente, B. Ryffel, and I. Couillin. 2007. Il-1r1/myd88 signaling and the inflammasome are essential in pulmonary inflammation and fibrosis in mice. *J. Clin. Invest.* 117:3786–3799.

Gavett, S. H., C. U. Parkinson, G. A. Willson, C. E. Wood, A. M. Jarabek, K. C. Roberts, U. P. Kodavanti, and D. E. Dodd. 2016. Persistent effects of libby amphibole and amosite asbestos following subchronic inhalation in rats. *Part Fibre Toxicol.* 13:17.

Gharaee-Kermani, M., Y. Nozaki, K. Hatano, and S. H. Phan. 2001. Lung interleukin-4 gene expression in a murine model of bleomycin-induced pulmonary fibrosis. *Cytokine* 15:138–147.

Ghio, A., R. J. Tan, K. Ghio, C. L. Fattman, and T. D. Oury. 2009. Iron accumulation and expression of iron-related proteins following murine exposure to crocidolite. *J. Environ. Pathol. Toxicol. Oncol.* 28:153–162.

Ghio, A. J. 2009. Disruption of iron homeostasis and lung disease. *Biochim. Biophys. Acta.* 1790:731–739.

Goodglick, L. A., and A. B. Kane. 1986. Role of reactive oxygen metabolites in crocidolite asbestos toxicity to mouse macrophages. *Cancer Res.* 46:5558–5566.

Governa, M., L. Camilucci, M. Amati, I. Visona, M. Valentino, G. C. Botta, A. Campopiano, and C. Fanizza. 1998. Wollastonite fibers in vitro generate reactive oxygen species able to lyse erythrocytes and activate the complement alternate pathway. *Toxicol. Sci.* 44:32–38.

Gualtieri, A. F., N. Bursi Gandolfi, S. Pollastri, M. Burghammer, E. Tibaldi, F. Belpoggi, K. Pollok, F. Langenhorst, R. Vigliaturo, and G. Drazic. 2017. New insights into the toxicity of mineral fibres: A combined in situ synchrotron MU-XRD and HR-TEM study of chrysotile, crocidolite, and erionite fibres found in the tissues of Sprague-Dawley rats. *Toxicol. Lett.* 274:20–30.

Harper, M., B. Van Gosen, O. S. Crankshaw, S. S. Doorn, T. J. Ennis, and S. E. Harrison. 2015. Characterization of lone pine, California, tremolite asbestos and preparation of research material. *Ann. Occup. Hyg.* 59:91–103.

Hillegass, J. M., A. Shukla, S. A. Lathrop, M. B. MacPherson, S. L. Beuschel, K. J. Butnor, J. R. Testa, H. I. Pass, M. Carbone, C. Steele, and B. T. Mossman. 2010. Inflammation precedes the development of human malignant mesotheliomas in a SCID mouse xenograft model. *Ann. N Y Acad. Sci.* 1203:7–14.

Kamp, D. W., E. Shacter, and S. A. Weitzman. 2011. Chronic inflammation and cancer: The role of the mitochondria. *Oncology* 25 (400–410):413.

Kane, A. B. 1996. Mechanisms of mineral fibre carcinogenesis. *IARC Sci. Publ.* 11–34.

Kuleshov, M. V., M. R. Jones, A. D. Rouillard, N. F. Fernandez, Q. Duan, Z. Wang, S. Koplev, S. L. Jenkins, K. M. Jagodnik, A. Lachmann, M. G. McDermott, C. D. Monteiro, G. W. Gundersen, and A. Ma'ayan. 2016. Enrichr: A comprehensive gene set enrichment analysis web server 2016 update. *Nucl. Acids. Res.* 44:W90–W97.

LaDou, J., B. Castleman, A. Frank, M. Gochfeld, M. Greenberg, J. Huff, T. K. Joshi, P. J. Landrigan, R.

Downloaded by [Stephen B. Thacker CDC Library] at 09:00 11 January 2018

Lemen, J. Myers, M. Soffritti, C. L. Soskolne, K. Takahashi, D. Teitelbaum, B. Terracini, and A. Watterson. 2010. The case for a global ban on asbestos. *Environ. Health Persp.* 118:897–901.

Lemen, R. A. 2016. Mesothelioma from asbestos exposures: Epidemiologic patterns and impact in the united states. *J. Toxicol. Environ. Health B* 19:250–265.

Li, W. 2012. Volcano plots in analyzing differential expressions with mrna microarrays. *J. Bioinform. Comput. Biol.* 10:1231003.

Lowers, H., and G. Meeker. 2002. Tabulation of asbestos-related terminology. In *Open-file report (Report 02-458). U.S. geological survey*., Version 1.0. http://pubs.er.usgs.gov/publication/ofr02458.

Lowers, H. A., D. T. Adams, G. P. Meeker, and C. J. Nutt. 2010. *Chemical and morphological comparison of erionite from Oregon, North Dakota, and Turkey*. Reston, VA: Environmental Protection Agency, Denver, CO. Region VIII.; Geological Survey.

Mastruzzo, C., N. Crimi, and C. Vancheri. 2002. Role of oxidative stress in pulmonary fibrosis. *Monaldi Arch. Chest. Dis.* 57:173–176.

Maxim, L. D., and E. E. McConnell. 2005. A review of the toxicology and epidemiology of wollastonite. *Inhal. Toxicol.* 17:451–466.

McConnell, E. E., L. Hall, and B. Adkins. 1991. Studies on the chronic toxicity (inhalation) of wollastonite in fischer 344 rats. *Inhal. Toxicol.* 3:323–337.

Moller, P., P. H. Danielsen, D. G. Karottki, K. Jantzen, M. Roursgaard, H. Klingberg, D. M. Jensen, D. V. Christophersen, J. G. Hemmingsen, Y. Cao, and S. Loft. 2014. Oxidative stress and inflammation generated DNA damage by exposure to air pollution particles. *Mutat. Res. Rev. Mutat. Res.* 762:133–166.

Mossman, B. T., and A. Churg. 1998. Mechanisms in the pathogenesis of asbestosis and silicosis. *Am. J. Respir. Crit. Care Med.* 157:1666–1680.

Mossman, B. T., and J. P. Marsh. 1989. Evidence supporting a role for active oxygen species in asbestos-induced toxicity and lung disease. *Environ. Health Persp.* 81:91–94.

Murray, A. R., E. R. Kisin, A. V. Tkach, N. Yanamala, R. Mercer, S. H. Young, B. Fadeel, V. E. Kagan, and A. A. Shvedova. 2012. Factoring-in agglomeration of carbon nanotubes and nanofibers for better prediction of their toxicity versus asbestos. *Part Fibre Toxicol.* 9:10.

Murtagh, F., and P. Legendre. 2014. Ward's hierarchical agglomerative clustering method: Which algorithms implement ward's criterion? *J. Classif.* 31:274–295.

National Research Council (U.S.). Committee on Nonoccupational Health Risks of Asbestiform Fibers. 1984. *Asbestiform fibers: Nonoccupational health risks*. Washington, D.C.: National Academy Press.

Ndlovu, N., D. Rees, J. Murray, N. Vorajee, G. Richards, and J. teWaterNaude. 2017. Asbestos-related diseases in mineworkers: A clinicopathological study. *ERJ Open Res.* 3. http://openres.ersjournals.com/content/erjor/3/3/00022-2017.full.pdf

Noonan, C. W., J. C. Pfau, T. C. Larson, and M. R. Spence. 2006. Nested case-control study of autoimmune disease in an asbestos-exposed population. *Environ. Health Persp.* 114:1243–1247.

NTP. 2016. Asbestos. In *Report on carcinogens*, 14th ed. Research Triangle Park, NC: U.S. Department of Health and Human Services, Public Health Service. http://ntp.niehs.nih.gov/go/roc14/.

Nymark, P., P. M. Lindholm, M. V. Korpela, L. Lahti, S. Ruosaari, S. Kaski, J. Hollmen, S. Anttila, V. L. Kinnula, and S. Knuutila. 2007. Gene expression profiles in asbestos-exposed epithelial and mesothelial lung cell lines. *BMC Genomics.* 8:62.

O'Reilly, K. M., A. M. McLaughlin, W. S. Beckett, and P. J. Sime. 2007. Asbestos-related lung disease. *Am. Family Physician.* 75:683–688.

Oberdorster, G. 1996. Evaluation and use of animal models to assess mechanisms of fibre carcinogenicity. *IARC Sci. Publ.* 140:107–125.

Ogushi, F. 1996. The role of cytokines in pulmonary fibrosis. *Nihon Ika Daigaku Zasshi* 63:391–394.

Palekar, L. D., J. F. Eyre, B. M. Most, and D. L. Coffin. 1987. Metaphase and anaphase analysis of v79 cells exposed to erionite, UICC chrysotile and UICC crocidolite. *Carcinogenesis* 8:553–560.

Palekar, L. D., B. M. Most, and D. L. Coffin. 1988. Significance of mass and number of fibers in the correlation of V79 cytotoxicity with tumorigenic potential of mineral fibers. *Environ. Res.* 46:142–152.

Pascolo, L., G. Zabucchi, A. Gianoncelli, G. Kourousias, E. Trevisan, E. Pascotto, C. Casarsa, C. Ryan, M. Lucattelli, G. Lungarella, E. Cavarra, B. Bartalesi, M. Zweyer, F. Cammisuli, M. Melato, and V. Borelli. 2016. Synchrotron x-ray microscopy reveals early calcium and iron interaction with crocidolite fibers in the lung of exposed mice. *Toxicol. Lett.* 241:111–120.

Pfau, J. C., K. M. Serve, and C. W. Noonan. 2014. Autoimmunity and asbestos exposure. *Autoimmune. Dis.* 2014:782045.

Pinkerton, K. E., S. L. Young, E. K. Fram, and J. D. Crapo. 1990. Alveolar type ii cell responses to chronic inhalation of chrysotile asbestos in rats. *Am. J. Respir. Cell. Mol. Biol.* 3:543–552.

Poland, C. A., R. Duffin, I. Kinloch, A. Maynard, W. A. Wallace, A. Seaton, V. Stone, S. Brown, W. Macnee, and K. Donaldson. 2008. Carbon nanotubes introduced into the abdominal cavity of mice show asbestos-like pathogenicity in a pilot study. *Nat. Nanotechnol.* 3:423–428.

Pollastri, S., A. F. Gualtieri, R. Vigliaturo, K. Ignatyev, E. Strafella, A. Pugnaloni, and A. Croce. 2016. Stability of mineral fibres in contact with human cell cultures. An in situ muxanes, muxrd and xrf iron mapping study. *Chemosphere* 164:547–557.

Quinlan, T. R., K. A. BeruBe, J. P. Marsh, Y. M. Janssen, P. Taishi, K. O. Leslie, D. Hemenway, P. T. O'Shaughnessy, P. Vacek, and B. T. Mossman. 1995. Patterns of inflammation, cell proliferation, and related gene expression in lung

after inhalation of chrysotile asbestos. *Am. J. Pathol.* 147:728–739.

R Development Core Team. (2010). R: A language and environment for statistical computing. R Foundation for Statistical Computing, Vienna, Austria. URL. http://www.R-project.org/.

Ramos-Nino, M. E., C. R. Timblin, and B. T. Mossman. 2002. Mesothelial cell transformation requires increased AP-1 binding activity and ERK-dependent FRA-1 expression. *Cancer Res.* 62:6065–6069.

Rao, G. V., S. Tinkle, D. N. Weissman, J. M. Antonini, M. L. Kashon, R. Salmen, L. A. Battelli, P. A. Willard, M. D. Hoover, and A. F. Hubbs. 2003. Efficacy of a technique for exposing the mouse lung to particles aspirated from the pharynx. *J. Toxicol. Environ. Health A* 66:1441–1452.

Roe, O. D., E. Anderssen, E. Helge, C. H. Pettersen, K. S. Olsen, H. Sandeck, R. Haaverstad, S. Lundgren, and E. Larsson. 2009. Genome-wide profile of pleural mesothelioma versus parietal and visceral pleura: The emerging gene portrait of the mesothelioma phenotype. *PLoS One* 4:e6554.

Rola-Pleszczynski, M., S. Gouin, and R. Begin. 1984. Asbestos-induced lung inflammation. Role of local macrophage-derived chemotactic factors in accumulation of neutrophils in the lungs. *Inflammation* 8:53–62.

Sanchez, V. C., J. R. Pietruska, N. R. Miselis, R. H. Hurt, and A. B. Kane. 2009. Biopersistence and potential adverse health impacts of fibrous nanomaterials: What have we learned from asbestos? *Wiley Interdiscip. Rev. Nanomed. Nanobiotechnol.* 1:511–529.

Sayan, M., and B. T. Mossman. 2016. The nlrp3 inflammasome in pathogenic particle and fibre-associated lung inflammation and diseases. *Part Fibre Toxicol.* 13:51.

Searl, A., D. Buchanan, R. T. Cullen, A. D. Jones, B. G. Miller, and C. A. Soutar. 1999. Biopersistence and durability of nine mineral fibre types in rat lungs over 12 months. *Ann. Occup. Hyg.* 43:143–153.

Shatos, M. A., J. M. Doherty, J. P. Marsh, and B. T. Mossman. 1987. Prevention of asbestos-induced cell death in rat lung fibroblasts and alveolar macrophages by scavengers of active oxygen species. *Environ. Res.* 44:103–116.

Shukla, A., J. M. Miller, C. Cason, M. Sayan, M. B. MacPherson, S. L. Beuschel, J. Hillegass, P. M. Vacek, H. I. Pass, and B. T. Mossman. 2013. Extracellular signal-regulated kinase 5: A potential therapeutic target for malignant mesotheliomas. *Clin. Cancer Res.* 19:2071–2083.

Singh, A., N. Pruett, and C. D. Hoang. 2017. In vitro experimental models of mesothelioma revisited. *Transl. Lung Cancer Res.* 6:248–258.

Tatrai, E., M. Brozik, Z. Kovacikova, and M. Horvath. 2005. The effect of asbestos and stone-wool fibres on some chemokines and redox system of pulmonary alveolar macrophages and pneumocytes type II. *Biomed. Pap. Med. Fac. Univ. Palacky Olomouc Czech Repub.* 149:357–361.

Trevisan, E., G. Zabucchi, L. Pascolo, E. Pascotto, C. Casarsa, M. Lucattelli, G. Lungarella, E. Cavarra, B. Bartalesi, M. Zweyer, and V. Borelli. 2016. Histopathological data of iron and calcium in the mouse lung after asbestos exposure. *Data Brief* 6:769–775.

Wagner, J. C., J. W. Skidmore, R. J. Hill, and D. M. Griffiths. 1985. Erionite exposure and mesotheliomas in rats. *Br. J. Cancer* 51:727–730.

Ward, J. H. 1963. Hierarchical grouping to optimize an objective function. *J. Am. Stat. Assoc.* 58:236–244.

Wild, P. 2006. Lung cancer risk and talc not containing asbestiform fibres: A review of the epidemiological evidence. *Occup. Environ. Med.* 63:4–9.

Williams, P. R., A. D. Phelka, and D. J. Paustenbach. 2007. A review of historical exposures to asbestos among skilled craftsmen (1940-2006). *J. Toxicol. Environ. Health B.* 10:319–377.

Wylie, A. G., and P. A. Candela. 2015. Methodologies for determining the sources, characteristics, distribution, and abundance of asbestiform and nonasbestiform amphibole and serpentine in ambient air and water. *J. Toxicol. Environ. Health B.* 18:1–42.

Wynn, T. A. 2008. Cellular and molecular mechanisms of fibrosis. *J. Pathol.* 214:199–210.

Zabeau, L., P. Gevaert, C. Bachert, and J. Tavernier. 2003. Interleukin-5, eosinophilic diseases and therapeutic intervention. *Curr. Drug Targets Inflamm. Allergy.* 2:319–328.

Zhang, K., and S. H. Phan. 1996. Cytokines and pulmonary fibrosis. *Biol. Sig.* 5:232–239.

Zhu, Z., R. J. Homer, Z. Wang, Q. Chen, G. P. Geba, J. Wang, Y. Zhang, and J. A. Elias. 1999. Pulmonary expression of interleukin-13 causes inflammation, mucus hypersecretion, subepithelial fibrosis, physiologic abnormalities, and eotaxin production. *J. Clin. Invest.* 103:779–788.

Zurawski, G., and J. E. De Vries. 1994. Interleukin 13, an interleukin 4-like cytokine that acts on monocytes and b cells, but not on t cells. *Immunol. Today* 15:19–26.

Downloaded by [Stephen B. Thacker CDC Library] at 09:00 11 January 2018